Biophysical Journal Volume 108 May 2015 2212–2222

Article

Ordered Raft Domains Induced by Outer Leaflet Sphingomyelin in Cholesterol-Rich Asymmetric Vesicles

Qingqing Lin[1] and Erwin London[1,*]
[1]Department of Biochemistry and Cell Biology, Stony Brook University, Stony Brook, New York

ABSTRACT Sphingolipid- and cholesterol-rich liquid-ordered (Lo) lipid domains (rafts) are thought to be important organizing elements in eukaryotic plasma membranes. How they form in the sphingolipid-poor cytosolic (inner) membrane leaflet is unclear. Here, we characterize how outer-leaflet Lo domains induce inner-leaflet-ordered domains, i.e., interleaflet coupling. Asymmetric vesicles studied contained physiologically relevant cholesterol levels (~37 mol %), a mixture of SM (sphingomyelin) and DOPC (dioleoylphosphatidylcholine) in their outer leaflets, and DOPC in their inner leaflets. Lo domains were observed in both leaflets, and were in register, indicative of coupling between SM-rich outer-leaflet-ordered domains and inner-leaflet-ordered domains. For asymmetric vesicles with outer-leaflet egg SM or milk SM, a fluorescent lipid with unsaturated acyl chains (NBD-DOPE) was depleted in both the outer- and inner-leaflet-ordered domains. This suggests the inner-leaflet-ordered domains were depleted in unsaturated lipid (i.e., DOPC) and thus rich in cholesterol. For asymmetric vesicles containing egg SM, outer-leaflet Lo domains were also depleted in a saturated fluorescent lipid (NBD-DPPE), while inner-leaflet Lo domains were not. This indicates that inner- and outer-leaflet Lo domains can have significantly different physical properties. In contrast, in asymmetric vesicles containing outer-leaflet milk SM, which has long acyl chains capable of interdigitating into the inner leaflet, both outer- and inner-leaflet Lo domains were depleted, to a similar extent, in NBD-DPPE. This is indicative of interdigitation-enhanced coupling resulting in inner- and outer-leaflet Lo domains with similar physical properties.

INTRODUCTION

Lipid asymmetry refers to the difference in lipid composition in the inner and outer monolayers (leaflets) of the lipid bilayer of a membrane (1,2). It is a feature of most cell plasma membranes, and may strongly influence membrane domain formation and lipid physical state. Plasma membranes are believed to contain lipid-ordered (Lo) domains rich in sphingolipids (which usually have saturated acyl chains) and cholesterol, often called "rafts", that coexist with liquid-disordered (Ld) domains rich in unsaturated lipids (3). Sphingolipids are rich in the exofacial (outer) leaflet of membranes, but are largely absent in the cytofacial (inner) leaflet (4). This raises an important question: how are domains organized in the inner leaflet? The answer may be that the outer-leaflet lipids forming Lo domains influence the physical properties of those inner-leaflet lipids with which they are in contact so as to induce inner-leaflet-ordered domain formation (5), i.e., that there is interleaflet coupling. In addition to our studies using asymmetric vesicles (see below), biophysical studies on both supported (6,7) and unsupported (8) asymmetric bilayers containing cholesterol have shown that under some conditions, ordered large-scale domain formation (phase separation) in one leaflet can induce phase separation in the other. These studies imply that interleaflet coupling can occur. Nevertheless, the details of how lipid structure influences interleaflet coupling, and under what conditions coupling is strong, remain largely unexplored.

To study this, we developed methods to prepare asymmetric lipid vesicles based on methyl-β-cyclodextrin-induced lipid exchange between vesicles having different lipid compositions (9,10). Asymmetric small unilamellar vesicles (SUVs), large unilamellar vesicles (LUVs), and giant unilamellar vesicles (GUVs) can be prepared (11–13). Studies in asymmetric SUVs and LUVs have defined what lipid compositions support lipid asymmetry, and have shown that asymmetric membranes with outer-leaflet sphingomyelin (SM) support the formation of the ordered state domains, at least in the outer leaflet, in the presence of inner leaflets composed of unsaturated lipids (9,10,12,13). In addition, in asymmetric GUVs lacking cholesterol, we found that the presence of outer-leaflet SM can reduce lateral diffusion in the inner leaflet (14).

Recently, employing lipid exchange induced by HPαCD (hydroxypropyl-α-cyclodextrin), we developed a method that allows facile control of cholesterol concentration in asymmetric LUV (15). Here, we adapt this method for use in GUV. We find here that in asymmetric vesicles containing ~37 mol % cholesterol, Lo domains in egg-SM- or in milk-SM-rich outer leaflets induce the formation of coupled ordered domains in inner leaflets containing DOPC, an unsaturated lipid ordinarily highly resistant to ordered domain formation. Interestingly, the partitioning behaviors

Submitted October 7, 2014, and accepted for publication March 23, 2015.
*Correspondence: erwin.london@stonybrook.edu
Editor: Kalina Hristova.

0006-3495/15/05/2212/11 $2.00
http://dx.doi.org/10.1016/j.bpj.2015.03.056

(i.e., relative affinities for ordered domains) of NBD-labeled lipids in the inner leaflet of vesicles with egg-SM-rich outer leaflets and vesicles containing the interdigitating lipid milk SM in their outer leaflet were different, implying that interleaflet acyl-chain interdigitation influences inner-leaflet physical properties. We discuss the basis by which ordered domains form in inner leaflets and its potential physiological implications.

MATERIALS AND METHODS

Materials

DOPC (1,2-dioleoyl-*sn*-glycero-3-phosphocholine), egg SM (sphingomyelin from chicken egg), milk SM (bovine), cholesterol, Rho-DOPE (1,2-dioleoyl-*sn*-glycero-3-phosphoethanolamine-N-(lissamine rhodamine B sulfonyl)), C_6-NBD-PC (1-palmitoyl-2-6-[(7-nitro-2-1,3-benzoxadiazol-4-yl)amino]-hexanoyl-phosphatidylcholine), NBD-DOPE (1,2-dioleoyl-*sn*-glycero-3-phosphoethanolamine-N-(7-nitro-2-1,3-benzoxadiazol-4-yl)), NBD-DPPE (1,2-dipalmitoyl-*sn*-glycero-3-phosphoethanolamine-N-(7-nitro-2-1,3-benzoxadiazol-4-yl)), NBD-DSPE (1,2-distearoyl-*sn*-glycero-3-phosphoethanolamine-N-(7-nitro-2-1,3-benzoxadiazol-4-yl)), and NBD-DPhPE (1,2-diphytanoyl-*sn*-glycero-3-phosphoethanolamine-N-(7-nitro-2-1,3-benzoxadiazol-4-yl)) were purchased from Avanti Polar Lipids (Alabaster, AL). Lipids were stored in chloroform at −20°C. Concentrations were determined by dry weight or by absorbance, using an ε of 95,000 cm^{-1} M^{-1} at 560 nm for rhodamine lipids in methanol or 21,000 cm^{-1} M^{-1} at 461 nm for NBD lipids in methanol (16). Trehalose dihydrate, HPαCD ((2-hydroxypropyl)-α-cyclodextrin), sodium dithionite (sodium hydrosulfite), and DPH (1,6-diphenyl-1,3,5-hexatriene) were purchased from Sigma-Aldrich (St. Louis, MO). PBS (10× phosphate-buffered saline, diluted to 1×; 10 mM sodium phosphate; and 150 mM sodium chloride, pH ~7.4) was purchased from Bio-Rad (Hercules, CA). High-performance thin-layer chromatography plates (Silica Gel 60) were purchased from VWR International (Batavia, IL).

Preparation of cholesterol-containing symmetric and asymmetric giant unilamellar vesicles (GUVs)

Symmetric GUVs were prepared as described in Chiantia et al. (17), while asymmetric GUVs were formed with a protocol adapted from Chiantia et al. (11). First, GUVs composed of 63:37 (mol/mol) DOPC/cholesterol labeled with 0.02 mol % of one fluorescently labeled lipid were prepared using the electroformation method (17). In general, lipids were dissolved in chloroform at 10 mg/mL, and a small volume (~1.2 μL) was spread on ITO-coated coverslips. The solvent was then completely evaporated, and the lipid-containing coverslip and a blank coverslip were then positioned in a home-built flow chamber at a distance of ~2 mm from each other. After, 200–300 μL trehalose solution (with the same osmolarity of the donor solutions, between 400 and 420 mOsm/kg, see below) was added to the chamber. (Trehalose was used to counterbalance the osmotic pressure at later stages of the process; it should be noted that trehalose may behave differently than other carbohydrates in terms of its interactions with lipid vesicles (18).) Next, a voltage of 1.2 V at 10 Hz was applied for at least 2 h at room temperature.

In a second step, donor vesicles containing the lipids to be delivered to the outer leaflet of GUVs were prepared. A quantity of 15 μmol donor lipids (in this case, 63:37 (mol/mol) egg SM/cholesterol, or 63:37 (mol/mol) milk SM/cholesterol, with 0.01 mol % fluorescently labeled lipid) were dried under nitrogen. Then the dried lipids were hydrated with 900 μL of 420 mM HPαCD at 70°C and diluted with 2.1 mL PBS. The sample was then incubated at 55°C and vortexed for at least 2 h. In order to remove any lipid aggregates and large MLVs, the donor mixture was then centrifuged at 16,000 × g for 15 min at room temperature (~23°C). Due to the high concentration of HPαCD, the lipid aggregates and large MLVs floated on the surface after centrifugation. The bottom clear solution that we refer to as "donor solution" was carefully removed and saved for the next step. The donor solution was shaken at 37°C until use. The osmolarity of the donor solution was between 400 and 420 mOsm/Kg (measured with a Micro-Osmometer 210; Advanced Instruments, Norwood, MA).

To initiate lipid exchange for the preparation of asymmetric GUVs, ~300 μL donor solution was injected into the GUV chamber and the chamber was placed on a 55°C hot plate. After 30 min at 55°C, the samples were gradually cooled down over a period of 10–15 min and delicately washed with 1 mL of the trehalose solution used in the first step.

In order to quench the NBD fluorescence in the outer leaflet of the asymmetric GUVs, ~300 μL of 1 mg/mL sodium dithionite (in Tris buffer pH 10, adjusted to a concentration of 400–420 mOsm/Kg with water to match the donor solution) was injected into the GUV chamber and incubated for 90 s. Then the sample was carefully washed with 2 mL of trehalose solution and imaged using confocal microscopy (within as little as 10 min and over a period of up to 2–3 h).

Preparation of cholesterol-containing asymmetric LUVs

Asymmetric LUVs were formed with a protocol adapted from Lin and London (15). First, acceptor vesicles, which form the inner-leaflet lipids of the asymmetric vesicles, were prepared. A quantity of 4 μmol lipids composed of 63:37 (mol/mol) DOPC/cholesterol were dried under nitrogen and followed by a high vacuum for at least 1 h. Then the dried lipids were dispersed in a 500-μL solution containing 25% (w/v) sucrose at 70°C. To obtain LUVs with a uniform size, the sample was subjected to seven cycles of freeze-and-thaw in a mixture of dry ice and acetone and then passed through 200-nm polycarbonate filters (Avanti Polar Lipids) 15 times. Next, the resulting LUVs were mixed with 3.5 mL PBS and subjected to ultracentrifugation at 190,000 × g at 25°C for 30 min. After the supernatant was discarded, the LUV pellet was resuspended with 500 μL PBS for later steps.

To prepare donor vesicles containing the lipids to be delivered to the outer leaflet of the LUVs, 8 μmol egg SM or milk SM were dried under nitrogen. The lipids were then hydrated with 450 μL PBS at 70°C and then mixed with 150 μL of 420 mM HPαCD. This donor mixture was placed in a multitube vortexer and vortexed at 55°C overnight.

The next day, the donor mixtures were added to 500 μL of acceptor LUVs prepared as above and vortexed at 55°C for 30 min. Next, the mixtures of donor (egg or milk) SM/HPαCD and acceptor DOPC/cholesterol LUVs were overlaid onto 3 mL of a 10% (w/v) sucrose solution, and subjected to ultracentrifugation at 190,000 × g, 25°C for 30 min. After the supernatant was removed, the resulting pellet was resuspended with 1 mL of 10% (w/v) sucrose solution and the ultracentrifugation step was repeated. The pellet was resuspended in PBS and immediately used for further experiments.

In some cases, when complete replacement of outer-leaflet DOPC with SM was desired, double-exchange was carried out. In a second round of exchange, pelleted vesicles from the above ultracentrifugation steps were resuspended with 500 μL PBS and mixed with another batch of the donor mixture. After incubation at 55°C for 30 min to carry out lipid exchange, two rounds of ultracentrifugation to wash away the donor vesicles were performed as above. The final pellet was resuspended in PBS and immediately used for further experiments.

Fluorescence imaging and quantitative analysis of asymmetric GUVs

Confocal imaging of GUVs was performed either on a ConfoCor 2 (Carl Zeiss, Jena, Germany) using a 40× water-immersion objective or on a

TCS SP5 (Leica Microsystems, Buffalo Grove, IL) with a CUBE & BOX temperature control system (Life Imaging Services, Basel, Switzerland) using a 40× oil-immersion objective. The sample was excited either by a 488-nm laser (green channel) for NBD-labeled lipids or a 543-nm laser (red channel) for rhodamine-labeled lipids. The fluorescence was then collected through either a 505–530 nm band-pass filter with a 70-μm pinhole for NBD-labeled lipids or a 585–615 nm band-pass filter with a 80-μm pinhole for rhodamine-labeled lipids. To avoid light-induced domain formation, a low-fluorescent probe concentration was used, and we did not see domain formation change during illumination. Unless otherwise noted, the measurements were performed on ConfoCor 2 confocal microscope (Carl Zeiss) at room temperature. To measure the temperature dependence of large domain formation, the measurements were performed on a TCS SP5 confocal microscope (Leica Microsystems) and the temperature of the samples was controlled by the CUBE & BOX system. Sample temperature was increased in steps, with micrographs recorded 1–2 min after the desired temperature was reached.

The apparent partition coefficient K (Lo/Ld) for NBD-labeled lipids between ordered and disordered domains was calculated from NBD intensity measurements in confocal sections of GUVs using a self-written algorithm routine in MATLAB (The MathWorks, Natick, MA) (19). For each combination of fluorescent labels (e.g., NBD-DOPE in the inner leaflet and Rho-DOPE in the outer leaflet) in GUVs, ~20–30 images, each of a different GUV, were taken and Rho-DOPE was used to mark the Ld phase. NBD intensity versus position was measured along a line of pixels perpendicular to the membrane plane. The line began outside the bilayer, intersected it, and then extended beyond. This allows determination of the background, which is subtracted from integrated intensity. This was repeated at 3–5 positions in an Lo and Ld domain to obtain a K_p value for a vesicle. The difference between NBD quantum yield in ordered and disordered domains was $<$10%, as judged by fluorescence in SM and DOPC LUV (data not shown), so data were not corrected from NBD quantum yield. NBD signals were weak, and therefore not corrected for pixel saturation. For each lipid/fluorescent probe composition, 3–5 sample preparations were carried out for asymmetric vesicles and two preparations for symmetric vesicles. We did not notice large differences in probe partition for different preparations of the same lipid mixture.

Other methods

The following methods were used as described elsewhere: high-performance thin-layer chromatography (12); lipid transverse diffusion measured by C_6-NBD-PC protection (9); dynamic light scattering (13); and steady-state fluorescence anisotropy (12).

RESULTS

Preparation of cholesterol-containing asymmetric GUVs

We produced cholesterol-containing asymmetric GUVs using cyclodextrin-mediated lipid exchange (11,15). HPαCD was used because it has no affinity for cholesterol, but maintains the ability to exchange phospholipids between vesicles (15). Before lipid exchange, the acceptor vesicles contained DOPC and 37 mol % cholesterol and the donor vesicles contained (egg or milk) SM and 37 mol % cholesterol. Also, before exchange one type of fluorescent lipid was present in (both leaflets of) the acceptor vesicles, and a second type of fluorescent lipid was present in (both leaflets of) the donor vesicles. After lipid exchange, the acceptor vesicles (some of which aggregate after lipid exchange) contain an outer leaflet composed of both DOPC and SM, an inner leaflet of DOPC, and cholesterol, which should be in both leaflets. The exact amount of SM in the outer leaflet was not determined, although it is very likely to be substantial, given the induction of ordered domain formation upon SM exchange. It should also be noted that HPαCD does not bind cholesterol, and no large-scale net delivery or removal of lipids has been observed in prior studies when carrying out HPαCD-catalyzed exchange (15). Thus, the cholesterol level is likely to remain close to 37 mol % after lipid exchange. However, cholesterol concentration still might decrease a small amount. Due to the tighter packing of SM relative to DOPC, to maintain a constant leaflet surface area SM might exchange with DOPC at $>$1:1. For replacement of one-half the outer-leaflet DOPC with SM, if the cross-sectional area of SM is only 75% that of DOPC, this might require an increase in total phospholipid + sphingolipid in the outer leaflet of ~12%, reducing outer-leaflet cholesterol to ~33 mol % and total cholesterol to 35 mol %. (Although differential affinity of unsaturated PC and SM should favor a higher concentration of cholesterol in the outer leaflet than in the inner leaflet, lipid balance requires close to equal cholesterol concentrations in each leaflet (15).)

After exchange, fluorescent lipids from the donor vesicles will now be present in the outer leaflet of the acceptor vesicles, while some of the outer-leaflet fluorescent lipids present in the acceptor vesicles before exchange will have been removed during exchange. Fluorescent lipids in the inner leaflet of the acceptor vesicles should not be transferred (15). To confirm this, as shown in Fig. 1, DOPC/cholesterol acceptor GUVs labeled with Rho-DOPE (*red*) acquired NBD-DOPE fluorescence (*green*) after lipid exchange, indicating that lipids from the donor vesicles were exchanged into acceptor GUVs. To confirm that lipids from donor vesicles were exchanged into the outer leaflet and not the inner leaflet, the relatively membrane-impermeable reagent sodium dithionite was introduced into the GUV chamber to destroy outer-leaflet NBD fluorescence. If any NBD-DOPE flipped into the inner leaflet, it would be protected from reduction by dithionite added to the external solution. Fig. 1 (*bottom panel*) shows that after a 90-s dithionite reduction step, for both vesicles with egg SM (Fig. 1 *A*) and milk SM (Fig. 1 *B*), little if any NBD fluorescence was detected. This indicates that lipids from donor vesicles were exchanged into the outer leaflet, suggesting that the GUVs are highly asymmetric.

The nomenclature we use for asymmetric vesicles with Lipid X and Y in the outer leaflet, Lipid Z in the inner leaflet, and cholesterol in both leaflets, is X + Y_o/Z_i/cholesterol.

To assess lipid asymmetry more quantitatively, LUVs were prepared using the same lipids and cholesterol concentrations (see Fig. S1 in the Supporting Material; and note that GUV cannot be used for these measurements). For egg SM + DOPCo/DOPCi/~37 mol % cholesterol

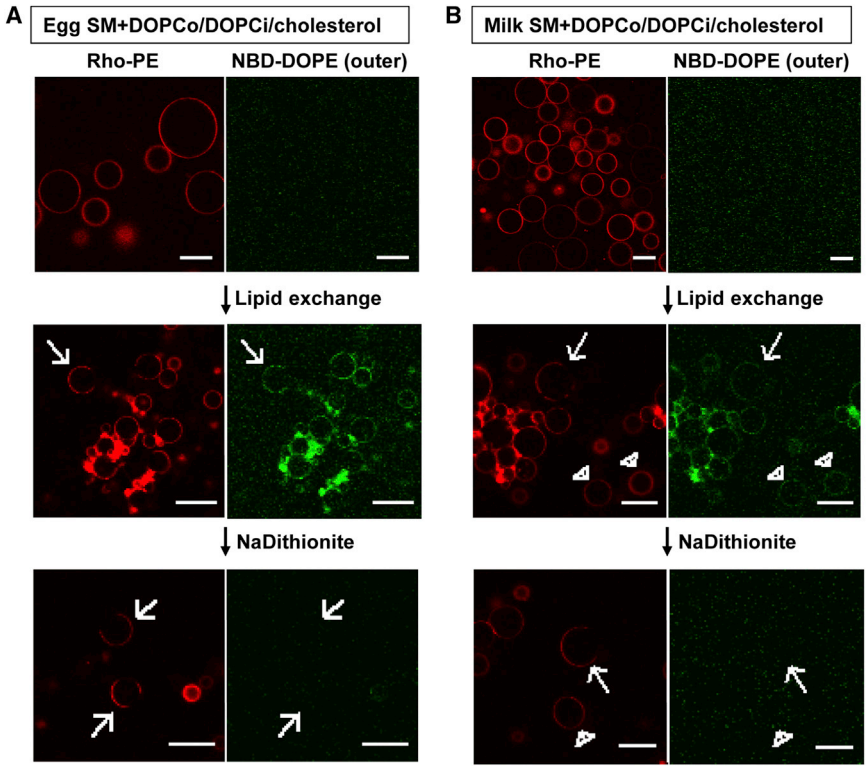

FIGURE 1 Preparation of SM + DOPCo/DOPCi/~37 mol % cholesterol vesicles. Asymmetric GUVs composed 37 mol % cholesterol and an inner leaflet of DOPC and an outer leaflet of egg SM (*A*) or milk SM (*B*) and DOPC. The acceptor vesicles were labeled with 0.02 mol % Rho-DOPE and the donor vesicles were labeled with 0.01 mol % NBD-DOPE. (*Top*) Before exchange. (*Middle*) After exchange. (*Bottom*) After lipid exchange and 1 mg/mL sodium dithionite added to destroy outer-leaflet NBD fluorescence. (*Arrows*) Vesicles with large-scale domain formation, which are the type of vesicles used for the later K_p analysis; (*arrow heads*) some homogeneous vesicles without domain formation. Vesicle positions are altered by dithionite addition and washing, so the *middle* and *bottom* panels do not represent the same vesicles. Scale bar = 20 μm. To see this figure in color, go online.

LUV, only ~2% of the NBD-PC initially introduced into the outer leaflet was protected from dithionite (i.e., likely located in the inner leaflet), and this only increased to 4% when the exchanged LUVs (after donor vesicle removal) were incubated overnight before dithionite treatment. This indicates that NBD-PC was distributed in the vesicles in a highly asymmetric fashion, and that its flip-flop was very slow in these vesicles, with a half-time no less than on the order of several days (Fig. S1, *B* and *C*). In contrast, in control LUV with NBD in both leaflets, as expected, ~50% of the NBD lipid fluorescence was protected from dithionite (Fig. S1, *D* and *E*). Assuming NBD-PC flip-flop is representative of that of the unlabeled lipids, this would be consistent with a highly asymmetric distribution of PC and SM.

To confirm asymmetry for the unlabeled lipid, we assessed SM asymmetry in LUV prepared using two rounds of lipid exchange to completely replace the outer-leaflet DOPC with egg or milk SM. Thin-layer chromatography (Fig. S2, *A* and *C*) confirmed that roughly half of DOPC was replaced by SM (52 ± 7% for egg PC, and 48 ± 6% for milk SM), and the fluorescence anisotropy of TMADPH introduced into the outer leaflet of the exchanged LUV was at least as high as that in SM/cholesterol vesicles, indicating the outer-leaflet DOPC had been virtually completely replaced by SM. Thus, there could be little if any SM in the inner leaflet, and the vesicles must have been fully or almost fully asymmetric (Fig. S2, *B* and *D*). Asymmetry was further confirmed by the difference between TMADPH anisotropy in these vesicles and in symmetric vesicles prepared from them by scrambling lipids (by solubilizing and then reforming vesicles as we previously published (12,13,15)) (Fig. S2, *B* and *D*). It should be emphasized that we have also observed stable asymmetry/slow flip-flop for vesicles with SM/DOPC mixtures in several prior studies, some with cholesterol, and that cholesterol slows flip-flop (9,12,15).

Domain formation (phase separation) and properties in symmetric vesicles

The domain-forming properties of symmetric and asymmetric GUVs containing SM, DOPC, and cholesterol were compared. To detect domains, two lipids that strongly prefer to locate in disordered (Ld) domains, Rho-DOPE and NBD-DOPE (20), were used. Thus, Ld domains appear relatively bright and Lo domains are relatively dark. To assess relative affinity of NBD-lipids for Lo domains, values of the partition coefficient, K_p, defined as the ratio of the concentration of a lipid in Lo domains relative to that in Ld domains, were estimated from the relative amount of NBD fluorescence in Lo and Ld domains. In other preparations, we examined the domain location of NBD-DPPE. NBD-DPPE, which has saturated acyl chains, generally has a higher affinity for ordered domains than NBD-DOPE (20).

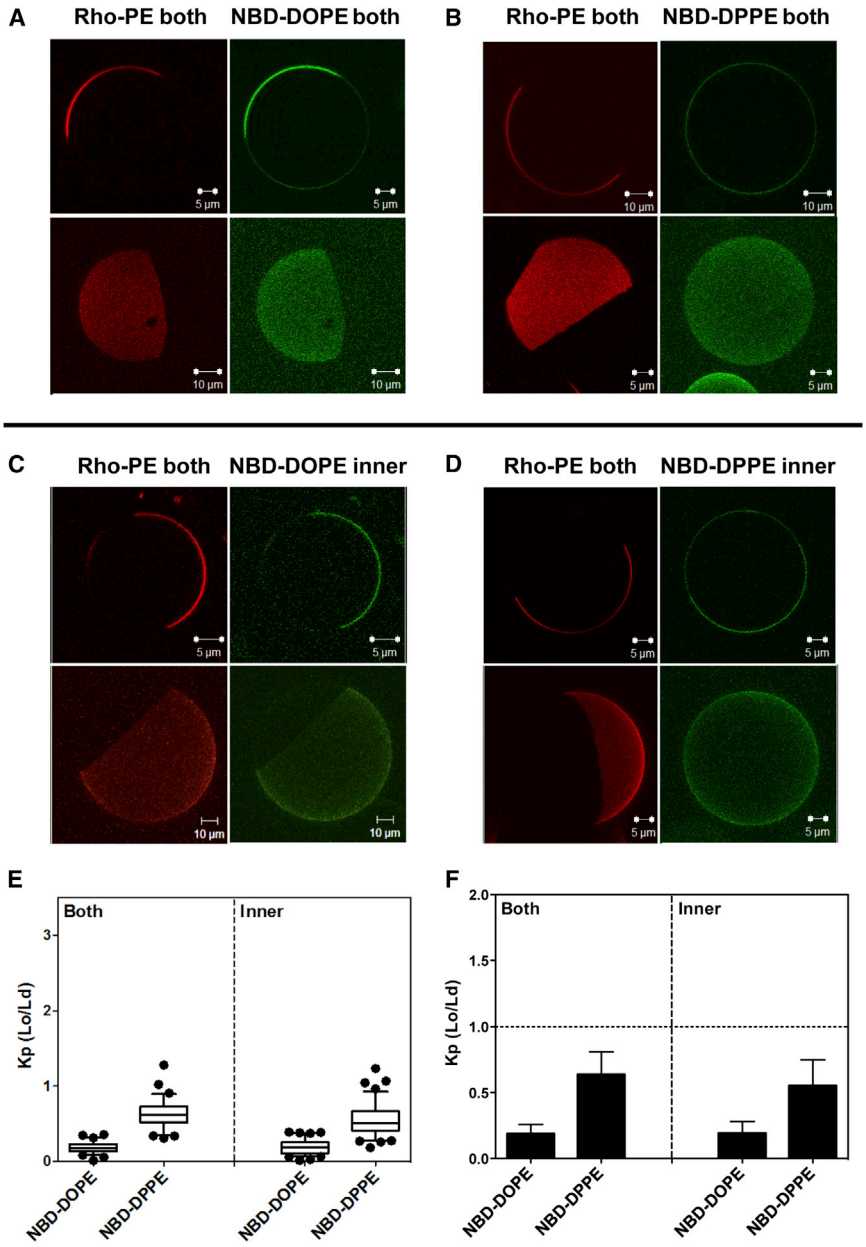

FIGURE 2 Images and NBD partition data for symmetric vesicles composed of 1:1 (mol/mol) egg SM/DOPC with 37 mol % cholesterol. Vesicles were labeled with Rho-DOPE and NBD-DOPE (*A*) or NBD-DPPE (*B*) in both leaflets or with Rho-DOPE in both leaflets and NBD-DOPE (*C*) or NBD-DPPE (*D*) in the inner leaflet. (Outer-leaflet NBD was reduced with sodium dithionite to restrict NBD fluorescence to the inner leaflet.) Two-dimensional cross-section images (*upper panels* in *A–D*) and three-dimensional reconstruction images (*bottom panels* in *A–D*) shown. The two- and three-dimensional images are from different vesicles. (*E* and *F*) Box plot and bar graph representations, respectively, of the NBD-DOPE and NBD-DPPE partition coefficient K_p (Lo/Ld). NBD-DOPE in both leaflets, $n = 21$; NBD-DOPE in the inner leaflet, $n = 27$; NBD-DPPE in both leaflets, $n = 27$; and NBD-DPPE in the inner leaflet, $n = 33$. The value of n here and below equals the number of vesicles analyzed. K_p (Lo/Ld) is the ratio of NBD fluorescence in Lo domains divided by that in Ld domains; K_p estimated here and in the following figures used intensity at 3–5 positions within Ld regions and 3–5 positions within Lo regions in each vesicle. To see this figure in color, go online.

The Rho-DOPE fluorescence in Fig. 2, *A* and *B*, shows that coexisting Lo and Ld domains/phases are present in symmetric GUVs composed of egg SM/DOPC/~37 mol % cholesterol. There were coexisting light and dark domains, implying that inner and outer leaflet domains were fully in register, i.e., coincident in location, such that Lo domains in one leaflet were in contact with Lo domains in the other leaflet. Because the fluorescent probes used were in both leaflets in this case, if domains had not been in register there would have been regions with intermediate fluorescence intensity, not just light and dark domains. Note the rounded domain shapes, indicative of liquid-liquid phase separation.

In these vesicles, NBD-DOPE fluorescence closely mirrored that of Rho-DOPE, as expected by its low tendency to partition into Lo domains, with a $K_p \sim 0.2$ (Fig. 2, *E* and *F*). In contrast, K_p values for NBD-DPPE were significantly higher (~0.65), as expected. It should be noted that due to high background values it is sometimes difficult to detect small differences in Ld and Lo NBD fluorescence intensities by eye.

Because the fluorescent probes were in both leaflets, these experiments show the average behavior of both leaflets. However, due to lipid symmetry, domains should have similar properties in both leaflets. Confirming this, K_p values for the NBD lipids were the same in vesicles before dithionite treatment (in which NBD fluorescence arose from both leaflets) and after destruction of outer-leaflet NBD groups with dithionite, in which case only

the inner-leaflet NBD lipid could be detected (Fig. 2, *C* and *D*).

Highly unsaturated inner leaflets composed of DOPC/cholesterol form domains (phase separate) in the presence of outer-leaflet egg SM

Next, domains/phase separation was evaluated in asymmetric egg SM + DOPCo/DOPCi/37 mol % cholesterol GUV (restricting analysis to vesicles that had not aggregated). Coexisting Lo and Ld domains formed in most of these vesicles (Fig. 3). (Vesicles lacking domains may reflect compositional heterogeneity or fission of vesicles with coexisting domains into pure Lo and pure Ld vesicles.) NBD-DOPE restricted to the outer leaflet confirmed the outer leaflet separated into coexisting Ld and Lo domains (Fig. 3 *A*), although NBD-DOPE was not as strongly excluded from Lo domains (see below) as in the symmetric vesicles. GUV with NBD-DOPE restricted to the inner leaflet (Fig. 3 *C*), showed that domain formation was also present in the inner leaflet, composed of DOPC and cholesterol. Furthermore, Rho-DOPE-rich Ld domains in the outer leaflet (Fig. 3 *C*) were coincident with NBD-DOPE-rich Ld domains in the inner leaflet (i.e., inner- and outer-leaflet Lo domains were coincident). This is indicative of interleaflet coupling in which inner-leaflet Lo domains are induced by

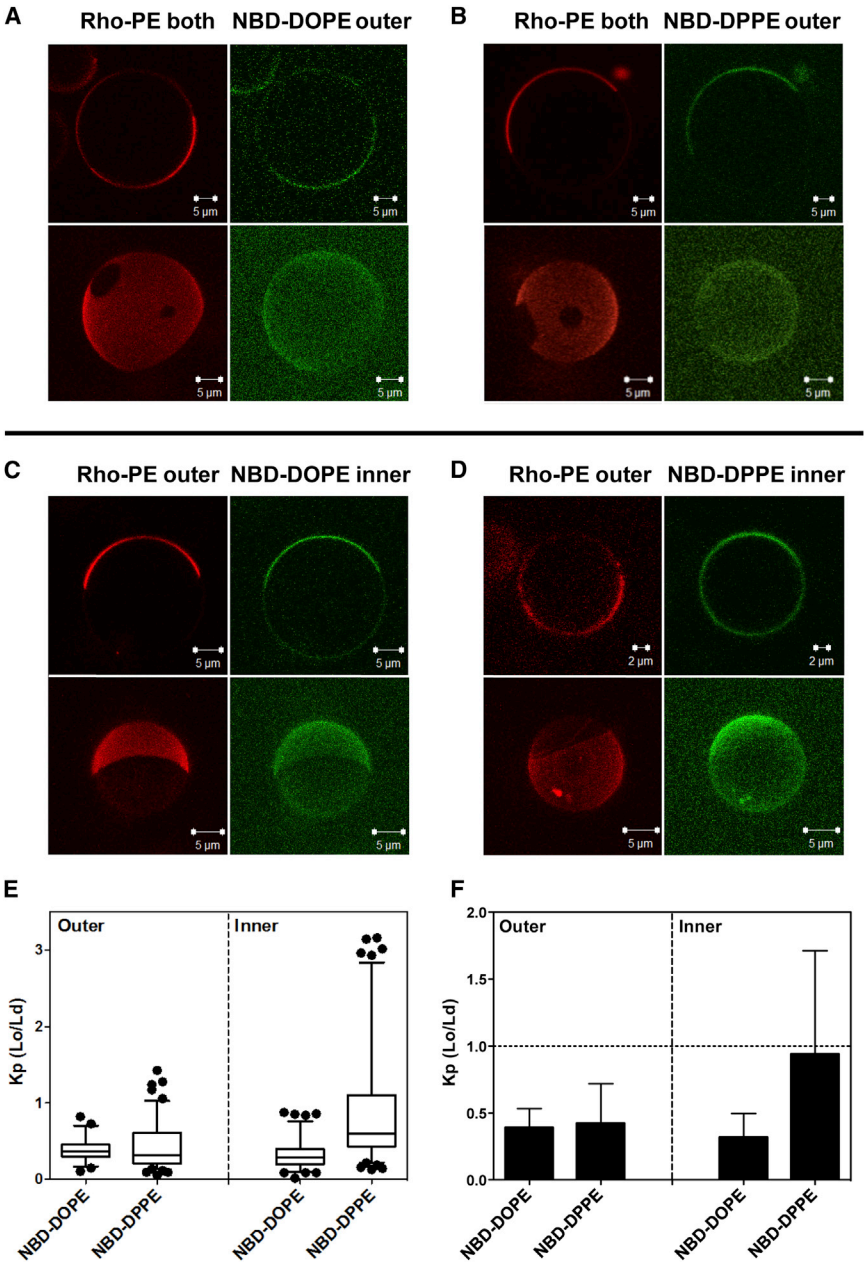

FIGURE 3 Images and NBD partition data for asymmetric egg SM + DOPCo/DOPCi/~37 mol % cholesterol GUV. GUV labeled with (*A*) NBD-DOPE or (*B*) NBD-DPPE in the outer leaflet, and labeled with NBD-DOPE (*C*) or with NBD-DPPE (*D*) in the inner leaflet. (*C* and *D*) To restrict NBD fluorescence to the inner leaflet, outer leaflet NBD was reduced with sodium dithionite. For GUV with outer-leaflet NBD lipid, Rho-DOPE was in both leaflets; for GUV with inner-leaflet NBD, lipid Rho-DOPE was exchanged into the outer leaflet. Note that the vesicles in (*D*) are from the less abundant subpopulation in which NBD-DPPE preferentially associates with Lo domains. (*A–D*) Two-dimensional cross-section images (*upper panel*) and three-dimensional reconstruction images (*bottom panel*) are shown. Two- and three-dimensional images are from different vesicles. (*E* and *F*) Box plot and bar graph representations, respectively, of NBD-DOPE and NBD-DPPE K_p (Lo/Ld). Box boundaries at 25% and 75% values, whiskers set at 5% and 95% values. NBD-DOPE in the outer leaflets, $n = 23$; NBD-DOPE in the inner leaflet, $n = 37$; NBD-DPPE in the outer leaflet, $n = 46$; NBD-DPPE in the inner leaflet, $n = 44$. To see this figure in color, go online.

outer-leaflet Lo domains. The affinity of NBD-DOPE for Ld domains relative to Lo domains was slightly weaker than that in symmetric vesicles. This was true both when the NBD-DOPE was in the inner and outer leaflets (Fig. 3, *E* and *F*).

A more complex partitioning pattern was observed for NBD-DPPE in egg SM + DOPCo/DOPCi/~37 mol% cholesterol asymmetric GUVs. Somewhat surprisingly, NBD-DPPE in the outer leaflet had a K_p value similar to that of NBD-DOPE, i.e., it tended to strongly localize in Ld domains (Fig. 3, *E* and *F*). In contrast, inner-leaflet NBD-DPPE had an affinity for Lo domains that was significantly higher than that in either the outer leaflet of the vesicles or symmetric vesicles. Inner-leaflet K_p values for NBD-DPPE were also relatively heterogeneous, with more vesicles having a $K_p < 1$ than $K_p > 1$ (Fig. 3 *E*), even though the average (mean) K_p was close to 1 (Fig. 3 *F*). On occasion, apparent inner-leaflet domain heterogeneity was observed in a single vesicle using NBD-DPPE. In contact with outer-leaflet Lo domains there would be both inner-leaflet domains in which NBD-DPPE was concentrated relative to Ld domains, and inner-leaflet regions in which NBD-DPPE levels were similar or identical to that in Ld domains (*lower two vesicles* in Fig. S3). The latter might be regions in which outer-leaflet Lo domains were in contact with inner-leaflet Ld domains, i.e., regions in which interleaflet coupling was lost, but this type of heterogeneity was never observed with NBD-DOPE partitioning. This suggests instead that two types of inner-leaflet Lo domains with subtly distinct properties can form, perhaps due to different degrees of interleaflet coupling.

To demonstrate these patterns were not specific to the particular choice of acyl chains on the NBD-labeled lipids chosen, partitioning behavior of two other NBD-labeled PE lipids was assessed in asymmetric and symmetric GUVs. NBD-DPhPE has several methyl groups on its acyl chains, and like NBD-DOPE cannot pack well with saturated lipids in ordered domains (21). It exhibited a behavior very similar to that of NBD-DOPE (Fig. S4). The ordered domain affinity of NBD-DSPE, which has saturated acyl chains but with two carbons longer than those of NBD-DPPE, was also studied. Its partitioning behavior was similar to that of NBD-DPPE (Fig. S5). Thus, the domain-forming and partitioning behavior observed was consistent with the properties of the NBD-lipid acyl chains.

Inner-leaflet-ordered domains (phases) induced by outer-leaflet milk SM differ from those formed by outer-leaflet egg SM

The effect of SM acyl-chain length/interdigitation upon interleaflet coupling was studied using milk SM. Milk SM acyl chains are predominantly significantly longer (i.e., C22:0 SM, C23:0 SM, and C24:0 SM) than those in egg SM (86% C16:0 SM) (22,23). Relative to the alkyl chain of the sphingoid base, the acyl chains of milk SM should protrude into the opposite leaflet, i.e., interdigitate. Large-scale phase separation was not observed in symmetric milk SM/DOPC/cholesterol GUVs, except at relatively low cholesterol concentrations (Fig. S6). However, as detected by the presence of coexisting membrane regions enriched and depleted in Rho-DOPE and NBD-DOPE, asymmetric milk SM + DOPCo/DOPCi/~37mol% cholesterol GUVs did form coexisting ordered domains and disordered domains (although with a little lower frequency than in vesicles formed from egg SM).

As in vesicles with egg SM, ordered domains were in registration in the inner and outer leaflets, indicative of interleaflet coupling in which outer-leaflet Lo domains induced formation of inner-leaflet Lo domains (Fig. 4, *A–D*). Unlike in asymmetric vesicles containing egg SM, both NBD-DOPE and NBD-DPPE partitioned favorably into Ld domains (as detected by being coincident with domains enriched in Rho-DOPE) in both the inner leaflet and outer leaflet (Fig. 4). NBD-DPPE had, at most, a slightly higher K_p for association with ordered domains than that of NBD-DOPE. Inner- and outer-leaflet K_p values were very similar for a given NBD-lipid. This is indicative of strong interleaflet coupling in which the physical properties of the inner and outer leaflet are similar (see the Discussion).

We also attempted to detect domains in vesicles containing brain SM. However, there was a lack of large-scale phase separation, at least in the large majority of asymmetric brain SM + DOPCo/DOPCi/~37 mol % cholesterol vesicles. This is not surprising, because lack of large-scale phase separation was also previously noted in brain SM + DOPCo/DOPCi/cholesterol vesicles (7,24).

Thermal stability of SM-induced inner-leaflet-ordered domains

In asymmetric GUVs composed of egg SM + DOPCo/DOPCi/~37 mol % cholesterol vesicles, large coexisting Lo and Ld domains were observed over a range of temperatures in both the outer (Rho-DOPE-labeled) and inner (NBD-DOPE-labeled) leaflet. When samples were heated, phase separation disappeared simultaneously in the inner and outer leaflet over a narrow temperature range (30–33°C) (Fig. 5 *A*). With asymmetric milk SM + DOPCo/DOPCi/~37 mol % cholesterol vesicles, large-scale phase separation also disappeared at higher temperatures (~36–39°C, Fig. S7).

DISCUSSION

The physical nature of inner-leaflet-ordered domains resulting from interleaflet coupling

It is a universal observation that ordered lipid domains tend to be depleted in unsaturated lipids and enriched in saturated

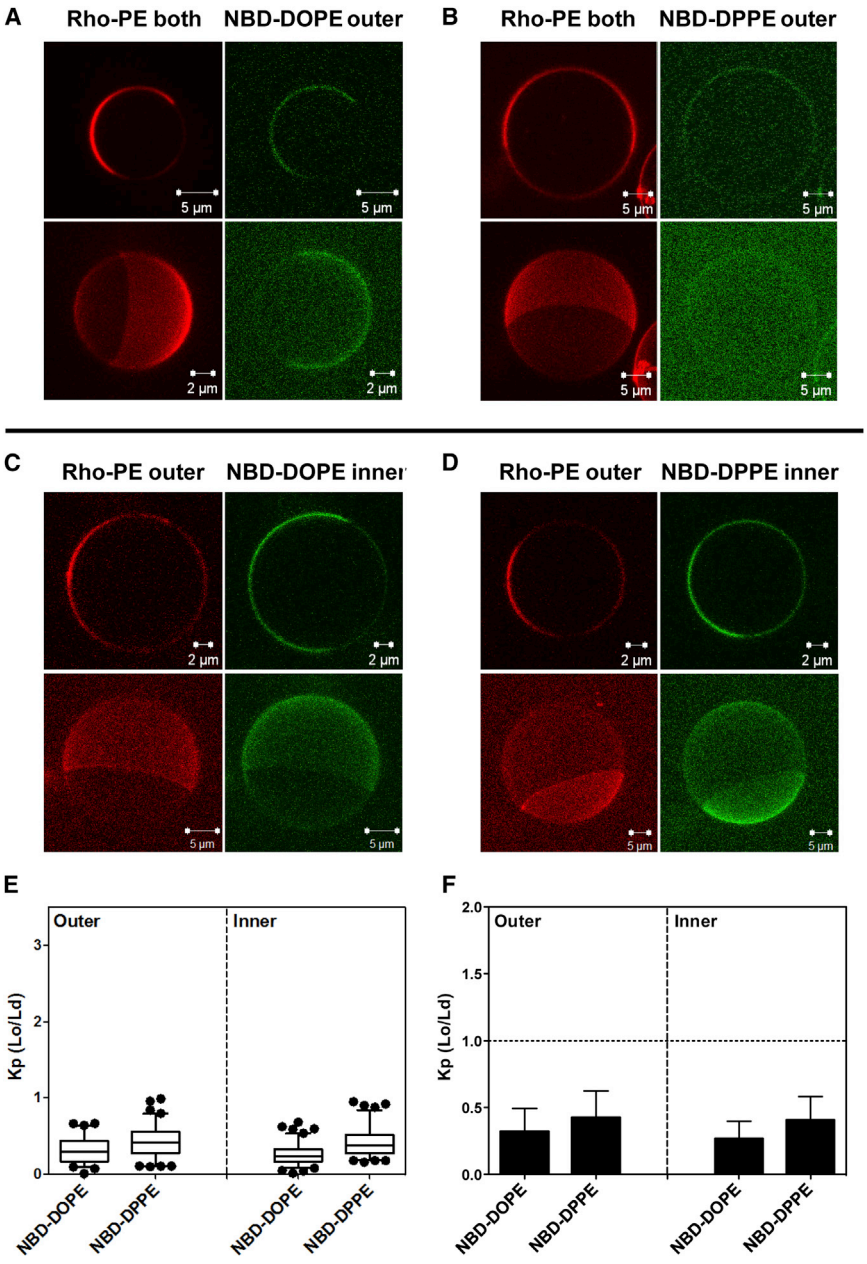

FIGURE 4 Images and NBD partition data for asymmetric milk SM + DOPCo/DOPCi/~37 mol % cholesterol GUV. GUV labeled with (*A*) NBD-DOPE or (*B*) NBD-DPPE in the outer leaflet, and with NBD-DOPE (*C*) or NBD-DPPE (*D*) in the inner leaflet. (*C* and *D*) To restrict NBD fluorescence to the inner leaflet, outer leaflet NBD was reduced with sodium dithionite. For GUV with outer-leaflet NBD lipid, Rho-DOPE was in both leaflets; for GUV with inner-leaflet NBD lipid, Rho-DOPE was exchanged into their outer leaflet. (*A–D*) Two-dimensional cross-section images (*upper panel*) and three-dimensional reconstruction images (*bottom panel*) were shown. Two- and three-dimensional images were taken from different vesicles except for (*B*), in which they are from the same vesicle to allow visualization of NBD partitioning. (*E* and *F*) Box plot and bar graph representations, respectively, of NBD-DOPE and NBD-DPPE K_p (Lo/Ld). NBD-DOPE in the outer leaflets, $n = 18$; NBD-DOPE in the inner leaflet, $n = 22$; NBD-DPPE in the outer leaflet, $n = 17$; NBD-DPPE in the inner leaflet, $n = 18$. To see this figure in color, go online.

lipids relative to coexisting disordered domains (3). Thus, the location of the saturated and unsaturated fluorescent lipids reveals that there are inner-leaflet-ordered domains, and they are in register with outer-leaflet Lo domains. This indicates that the outer-leaflet Lo domains that form upon introduction of SM into the outer leaflet induce formation of ordered domains in the inner leaflet. In other words, interleaflet coupling resulted in inner-leaflet phase separation.

Based on the differences in NBD-lipid K_p, it appears that the physical properties of ordered and disordered domains are not necessarily identical in the inner and outer leaflet. For example, in asymmetric vesicles with egg SM in the outer leaflet, K_p values for NBD-DPPE are higher in the inner leaflet than in the outer leaflet. This implies that there must be differences between lipid packing in inner- and outer-leaflet Lo domains, inner- and outer-leaflet Ld domains, or both inner- and outer-leaflet Ld and Lo domains, such that NBD-DPPE association with Lo domains is more favorable in the inner leaflet. If the partitioning of NBD-DPPE is reflective of packing in ordered domains, these results suggest Lo domains in the outer leaflet of the asymmetric vesicles are very tightly packed and NBD-DPPE partitions into them poorly. In contrast, Lo domains in the inner leaflet of the asymmetric vesicles may be less tightly packed than in the outer leaflet, so

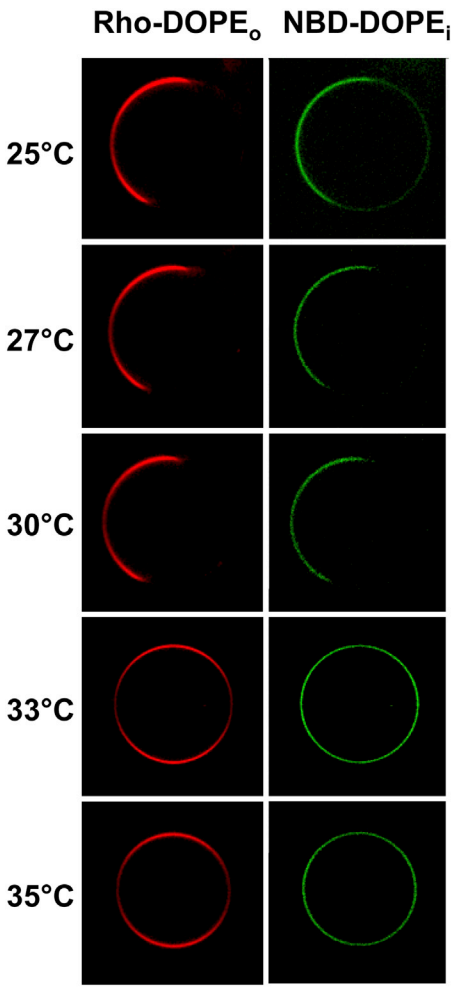

FIGURE 5 Thermal stability of large domains in egg SM + DOPCo/DOPCi/~37 mol % cholesterol GUVs. Acceptor vesicles contained 63:37 (mol/mol) DOPC/cholesterol labeled with NBD-DOPE. Donor vesicles contained 63:37 (mol/mol) egg SM/cholesterol labeled with Rho-DOPE. NBD in the outer leaflet was reduced with sodium dithionite for 90 s to restrict NBD fluorescence to the inner leaflet. Images were taken by the LAS AF confocal microscope (Leica Microsystems) with the CUBE & BOX temperature control system. Sample temperature was increased in steps taking a few minutes, with micrographs recorded 1–2 min after the desired temperature was reached. To see this figure in color, go online.

NBD-DPPE partitions into them more favorably. This behavior contrasts with both that in symmetric vesicles and that in asymmetric vesicles containing milk SM (see below), in which inner and outer leaflets domains may have nearly identical physical properties as judged from NBD-lipid partitioning.

Likely composition of inner-leaflet-ordered domains

A question arises from these studies: What is the composition of the inner-leaflet-ordered domains? Cholesterol tends to associate more strongly with ordered domains while DOPC tends to associate more strongly with disordered domains (3). Thus, because the inner leaflets contain DOPC and cholesterol, it is highly likely that inner-leaflet-ordered domains are enriched in cholesterol and depleted in DOPC relative to the remainder of the inner leaflet (i.e., the inner-leaflet-disordered domains). Depletion of DOPC within ordered domains would be consistent with the observed strong depletion of NBD-DOPE in ordered domains, because both DOPC and NBD-DOPE have oleoyl chains that resist association with ordered domains. We also cannot rule out the possibility that a small amount of SM reaches the inner leaflet and contributes to ordered domain formation in that leaflet.

Interestingly, if inner-leaflet-ordered domains arise from lateral rearrangement of DOPC and cholesterol in response to overlying outer-leaflet-ordered domains, then ordered inner-leaflet domains might not form when the entire outer leaflet is in the ordered state. In this case, there would be no lateral driving force for the lateral rearrangement of DOPC and cholesterol. Thus, a change in outer leaflets from all Lo to mixed Lo and Ld could trigger inner-leaflet Lo domain formation. If under basal conditions the outer leaflet of a plasma membrane was all in the Lo state, a decrease in outer-leaflet raft-forming lipids might trigger inner-leaflet raft formation in cells. This may have important biological implications. It is also possible an all-Ld lipid inner leaflet might force the outer leaflet to be fully in the disordered state, but this is not what we observe here, or in any of our previous studies of asymmetric vesicles.

Ordered domains can be formed by a phospholipid with a very low intrinsic ability to form ordered domains

DOPC has a very low tendency to form the ordered state membranes, as shown by pure DOPC vesicles having a melting temperature (T_m) for the solidlike gel to Ld transition at ~−20°C. This is as low as, or lower than, the T_m for the 1-acyl-chain-saturated, 2-acyl-chain-polyunsaturated lipids commonly found in mammalian membranes (25). Thus, the results in this report indicate that, at least at physiological cholesterol concentrations, interleaflet coupling is strong enough to force some lipids with a very low intrinsic tendency to form ordered domains to support ordered-domain formation when in contact with outer-leaflet-ordered domains.

In the pioneering study of Wan et al. (6) in planar bilayers it was demonstrated that coupling between ordered outer-leaflet domains (lower monolayer in the planar bilayer system) and inner-leaflet lipids could induce inner-leaflet-ordered domains when the outer leaflet contained lipids with saturated acyl chains (DPPC or SM) while the inner leaflet contained a mixture of natural inner-leaflet lipids. Coupling-induced inner-leaflet-ordered domains were observed for many different inner-leaflet

lipid compositions. However, ordered domains in a DOPC-containing leaflet were not prominent when the bilayers contained SM-rich outer-leaflet domains. This difference from our results may arise from a number of factors. First, the sample of Wan et al. (6) used a lower cholesterol concentration (20 mol %), and a different SM (brain SM) than used in our study. As noted above, we, and others (7), do not even see formation of large outer-leaflet domains in GUV with outer leaflets composed of brain SM and DOPC. Another difference was the incorporation in the SM-containing leaflet of planar bilayers of a few % of a cushioning PEG lipid, although this seems unlikely to have had much effect. Alternately, ordered domains may not have been detected in the planar bilayers due to a lack of fluorescence contrast between ordered and disordered domains. Ordered domains in Wan et al. (6) were detected with NBD-DPPE, which has an affinity for ordered domains that can be highly dependent upon their lipid composition, and when K_p is ~1 contrast is lost and it becomes difficult or impossible to detect domains. In fact, inspection of Fig. 2 in Wan et al. (6) does show faint evidence of domain formation in planar bilayers with 20 mol % cholesterol, and Wan et al. (6) did detect domain formation in leaflets containing other dioleoyl lipids when coupled to DPPC-containing ordered leaflets (6).

Effect of lipid interdigitation upon interleaflet coupling

We previously found in GUV-lacking cholesterol the presence of outer-leaflet lipids that can interdigitate into the inner leaflet (i.e., milk SM) induced interleaflet coupling that reduced the lateral diffusion of inner-leaflet DOPC (14), whereas egg SM did not. Here we find that in GUV containing cholesterol, the presence of outer-leaflet milk SM strengthened interleaflet coupling relative to egg SM, as judged by the similarity of inner- and outer-leaflet NBD-lipid K_p values. Thus, interdigitation seems to increase interleaflet coupling in general. This also suggests that the physical properties of the inner- and outer-leaflet domains are more similar with milk SM than in the case of inner- and outer-leaflet domains in vesicles containing egg SM, which should not interdigitate as much, if at all. Thus interdigitation and exact physical properties of inner-leaflet Lo and Ld domains may influence their affinity for specific proteins and lipids, and thus plasma membrane inner-leaflet structure and function. Consistent with this, a difference in the ability to interdigitate appears to have important biological consequences for the plasma membrane lipid LacCer (26).

SUPPORTING MATERIAL

Seven figures are available at http://www.biophysj.org/biophysj/supplemental/S0006-3495(15)00344-6.

ACKNOWLEDGMENTS

This work was supported by National Science Foundation grant No. DMR 1404985.

REFERENCES

1. Bretscher, M. S. 1972. Asymmetrical lipid bilayer structure for biological membranes. *Nat. New Biol.* 236:11–12.
2. Devaux, P. F. 1991. Static and dynamic lipid asymmetry in cell membranes. *Biochemistry.* 30:1163–1173.
3. Brown, D. A., and E. London. 1998. Structure and origin of ordered lipid domains in biological membranes. *J. Membr. Biol.* 164:103–114.
4. van Meer, G., D. R. Voelker, and G. W. Feigenson. 2008. Membrane lipids: where they are and how they behave. *Nat. Rev. Mol. Cell Biol.* 9:112–124.
5. Collins, M. D. 2008. Interleaflet coupling mechanisms in bilayers of lipids and cholesterol. *Biophys. J.* 94:L32–L34.
6. Wan, C., V. Kiessling, and L. K. Tamm. 2008. Coupling of cholesterol-rich lipid phases in asymmetric bilayers. *Biochemistry.* 47:2190–2198.
7. Visco, I., S. Chiantia, and P. Schwille. 2014. Asymmetric supported lipid bilayer formation via methyl-β-cyclodextrin mediated lipid exchange: influence of asymmetry on lipid dynamics and phase behavior. *Langmuir.* 30:7475–7484.
8. Collins, M. D., and S. L. Keller. 2008. Tuning lipid mixtures to induce or suppress domain formation across leaflets of unsupported asymmetric bilayers. *Proc. Natl. Acad. Sci. USA.* 105:124–128.
9. Son, M., and E. London. 2013. The dependence of lipid asymmetry upon phosphatidylcholine acyl chain structure. *J. Lipid Res.* 54:223–231.
10. Son, M., and E. London. 2013. The dependence of lipid asymmetry upon polar headgroup structure. *J. Lipid Res.* 54:3385–3393.
11. Chiantia, S., P. Schwille, …, E. London. 2011. Asymmetric GUVs prepared by MβCD-mediated lipid exchange: an FCS study. *Biophys. J.* 100:L1–L3.
12. Cheng, H. T., Megha, and E. London. 2009. Preparation and properties of asymmetric vesicles that mimic cell membranes: effect upon lipid raft formation and transmembrane helix orientation. *J. Biol. Chem.* 284:6079–6092.
13. Cheng, H. T., and E. London. 2011. Preparation and properties of asymmetric large unilamellar vesicles: interleaflet coupling in asymmetric vesicles is dependent on temperature but not curvature. *Biophys. J.* 100:2671–2678.
14. Chiantia, S., and E. London. 2012. Acyl chain length and saturation modulate interleaflet coupling in asymmetric bilayers: effects on dynamics and structural order. *Biophys. J.* 103:2311–2319.
15. Lin, Q., and E. London. 2014. Preparation of artificial plasma membrane mimicking vesicles with lipid asymmetry. *PLoS ONE.* 9:e87903.
16. Nelson, L. D., S. Chiantia, and E. London. 2010. Perfringolysin O association with ordered lipid domains: implications for transmembrane protein raft affinity. *Biophys. J.* 99:3255–3263.
17. Chiantia, S., N. Kahya, and P. Schwille. 2007. Raft domain reorganization driven by short- and long-chain ceramide: a combined AFM and FCS study. *Langmuir.* 23:7659–7665.
18. Madden, T. D., M. B. Bally, …, A. S. Janoff. 1985. Protection of large unilamellar vesicles by trehalose during dehydration: retention of vesicle contents. *Biochim. Biophys. Acta.* 817:67–74.
19. Lin, Q., and E. London. 2013. Altering hydrophobic sequence lengths shows that hydrophobic mismatch controls affinity for ordered lipid domains (rafts) in the multitransmembrane strand protein perfringolysin O. *J. Biol. Chem.* 288:1340–1352.
20. Sengupta, P., A. Hammond, …, B. Baird. 2008. Structural determinants for partitioning of lipids and proteins between coexisting fluid phases in giant plasma membrane vesicles. *Biochim. Biophys. Acta.* 1778:20–32.

21. Bakht, O., P. Pathak, and E. London. 2007. Effect of the structure of lipids favoring disordered domain formation on the stability of cholesterol-containing ordered domains (lipid rafts): identification of multiple raft-stabilization mechanisms. *Biophys. J.* 93:4307–4318.

22. Filippov, A., G. Orädd, and G. Lindblom. 2006. Sphingomyelin structure influences the lateral diffusion and raft formation in lipid bilayers. *Biophys. J.* 90:2086–2092.

23. Ramstedt, B., P. Leppimaki, …, J. P. Slotte. 1999. Analysis of natural and synthetic sphingomyelins using high-performance thin-layer chromatography. *Eur. J. Biochem./FEBS Lett.* 266:997–1002.

24. Petruzielo, R. S., F. A. Heberle, …, G. W. Feigenson. 2013. Phase behavior and domain size in sphingomyelin-containing lipid bilayers. *Biochim. Biophys. Acta.* 1828:1302–1313.

25. Koynova, R., and M. Caffrey. 1998. Phases and phase transitions of the phosphatidylcholines. *Biochim. Biophys. Acta.* 1376:91–145.

26. Sonnino, S., A. Prinetti, …, K. Iwabuchi. 2009. Role of very long fatty acid-containing glycosphingolipids in membrane organization and cell signaling: the model of lactosylceramide in neutrophils. *Glycoconj. J.* 26:615–621.

Supplementary Materials for "Ordered Raft Domains Induced by Outer Leaflet Sphingomyelin in Cholesterol-Rich Asymmetric Vesicles" Qingqing Lin and Erwin London*

Supplementary Figure 1. Analysis of lipid composition and asymmetry of LUV after one round of lipid exchange. (A) HP-TLC analysis of asymmetric egg SM+DOPCo/DOPCi/cholesterol LUVs prepared by a single exchange procedure. After exchange, acceptor LUVs are composed of 37 mol% cholesterol (based on initial lipid composition and assuming a lack of net lipid transfer (15)), an inner leaflet of DOPC and an outer leaflet of a mixture of egg SM and DOPC. (B) and (C) Measurement of lipid flip-flop in asymmetric egg SM+DOPCo/DOPCi/cholesterol LUVs by C_6-NBD-PC protection assay with 1 mol% C_6-NBD-PC relative to total lipids added externally to the vesicles. After 3h or overnight incubation, sodium dithionite was added to reduce outer leaflet NBD, and NBD fluorescence was measured as a function of time. Panel C. shows the percent protection derived from extrapolating percent protection to time zero after dithionite addition. (D) and (E) Measurement of lipid flip-flop in asymmetric egg SM+DOPCo/DOPCi/cholesterol LUVs by C_6-NBD-PC protection assay with C_6-NBD-PC incorporated into both inner and outer leaflets. Both donor and acceptor vesicles contained 1 mol% C_6-NBD-PC before exchange. Lipid exchange was carried out same as for samples without C_6-NBD-PC. After 3h or overnight incubation, sodium dithionite was added to reduce the NBD fluorescence. Panel E. shows the percent protection derived from extrapolating percent protection to time zero after dithionite addition. NBD protected is the fraction of NBD protected, which is the intensity of NBD fluorescence after exposure to dithionite divided by that before exposure to dithionite.

Supplementary Figure 2. Analysis of composition and asymmetry using LUV prepared by two rounds of lipid exchange. (A) and (B) HP-TLC analysis of asymmetric egg SMo/DOPCi/cholesterol LUVs (A) or milk SMo/DOPCi/cholesterol (B) prepared by a double exchange procedure. After two rounds of exchange, ~ 50 mol% of the non-cholesterol lipid in exchanged vesicles were SM. (C) TMADPH anisotropy of (left to right) symmetric egg SM/cholesterol, asymmetric egg SMo/DOPCi/cholesterol, scrambled vesicles, and symmetric DOPC/cholesterol at room temperature. (D) TMADPH anisotropy of (left to right) symmetric milk SM/cholesterol, asymmetric milk SMo/DOPCi/cholesterol, scrambled vesicles, and symmetric DOPC/cholesterol at room temperature. Cholesterol concentration (assuming no net lipid transfer) in all samples was 37 mol%. TMADPH dissolved in ethanol was added to preformed vesicles to a concentration of 0.1 mol% of total lipid. Samples were incubated for 10 min at room temperature before measurement. Average values (mean) and range are shown from duplicates for anisotropy measurements.

Supplementary Figure 3. Some representative vesicles illustrating the occasional (about one half of preparations) heterogeneity of NBD-DPPE partitioning in egg SM+DOPCo/DOPCi/cholesterol vesicles inner leaflet.

Supplementary Figure 4. (A) Confocal microscopic imaging of symmetric 1:1 egg SM/DOPC with 37 mol% cholesterol GUVs having both leaflets labeled with both Rho-DOPE and NBD-DPhPE (upper panel), asymmetric egg SM+DOPCo/DOPCi/~37 mol% cholesterol GUVs having inner leaflets labeled with NBD-DPhPE and outer leaflets labeled with Rho-DOPE (middle

panel), and asymmetric egg SM+DOPCo/DOPCi/~37 mol% cholesterol GUVs having both leaflets labeled with Rho-DOPE and outer leaflets labeled with NBD-DPhPE (bottom panel). (B) and (C) box plot and bar graph representations, respectively, of NBD-DPhPE partition coefficient, Kp (Lo/Ld). N=28 for NBD-DPhPE in symmetric vesicles both leaflets; n=19 for NBD-DPhPE in asymmetric vesicles outer leaflet and n=15 for NBD-DPhPE in asymmetric vesicles inner leaflet. Probe leaflet location: b=both; o=outer; i=inner

Supplementary Figure 5. (A) Confocal microscopic imaging of symmetric 1:1 (mol:mol) egg SM/DOPC with 37 mol% cholesterol GUVs having both leaflets labeled with both Rho-DOPE and NBD-DSPE (upper panel), asymmetric egg SM+DOPCo/DOPCi/~37 mol% cholesterol GUVs having inner leaflets labeled with NBD-DSPE and outer leaflets labeled with Rho-DOPE (middle panel), and asymmetric egg SM+DOPCo/DOPCi/~37 mol% cholesterol GUVs having both leaflets labeled with Rho-DOPE and outer leaflets labeled with NBD-DSPE (bottom panel). (B) and (C) box plot and bar graph representations, respectively, of NBD-DSPE partition coefficient, Kp (Lo/Ld). N=28 for NBD-DSPE in symmetric vesicles both leaflets; n=23 for NBD-DSPE in asymmetric vesicles outer leaflet and n=17 for NBD-DSPE in asymmetric vesicles inner leaflet. Probe leaflet location: b=both; o=outer; i=inner

Supplementary Figure 6. Domain formation in symmetric GUVs composed of 1:1 (mol:mol) milk SM/DOPC with different mol% of cholesterol. The vesicles were labeled with Rho-DOPE and NBD-DOPE in both leaflets. Left three panels: Rows from left to right are Rho-DOPE, NBD-DOPE and overlay. Right three panels: 3-D reconstructions. Rows from left to right are Rho-DOPE, NBD-DOPE and overlay.

Supplementary Figure 7. Thermal stability of large domains in milk SM+DOPCo/DOPCi/~37 mol% cholesterol GUVs. Acceptor vesicles contained 63:37 (mol:mol) DOPC/cholesterol labeled with NBD-DOPE. Donor vesicles contained 63:37 (mol:mol) milk SM/cholesterol labeled with Rho-DOPE. NBD in the outer leaflet was reduced with sodium dithionite for 90s to restrict NBD fluorescence to the inner leaflet. Images were taken by Leica LAS AF confocal microscope with the CUBE & BOX temperature control system. Sample temperature was increased in steps, with micrographs recorded 1-2 minutes after the desired temperature was reached.

Supplementary Figure 1

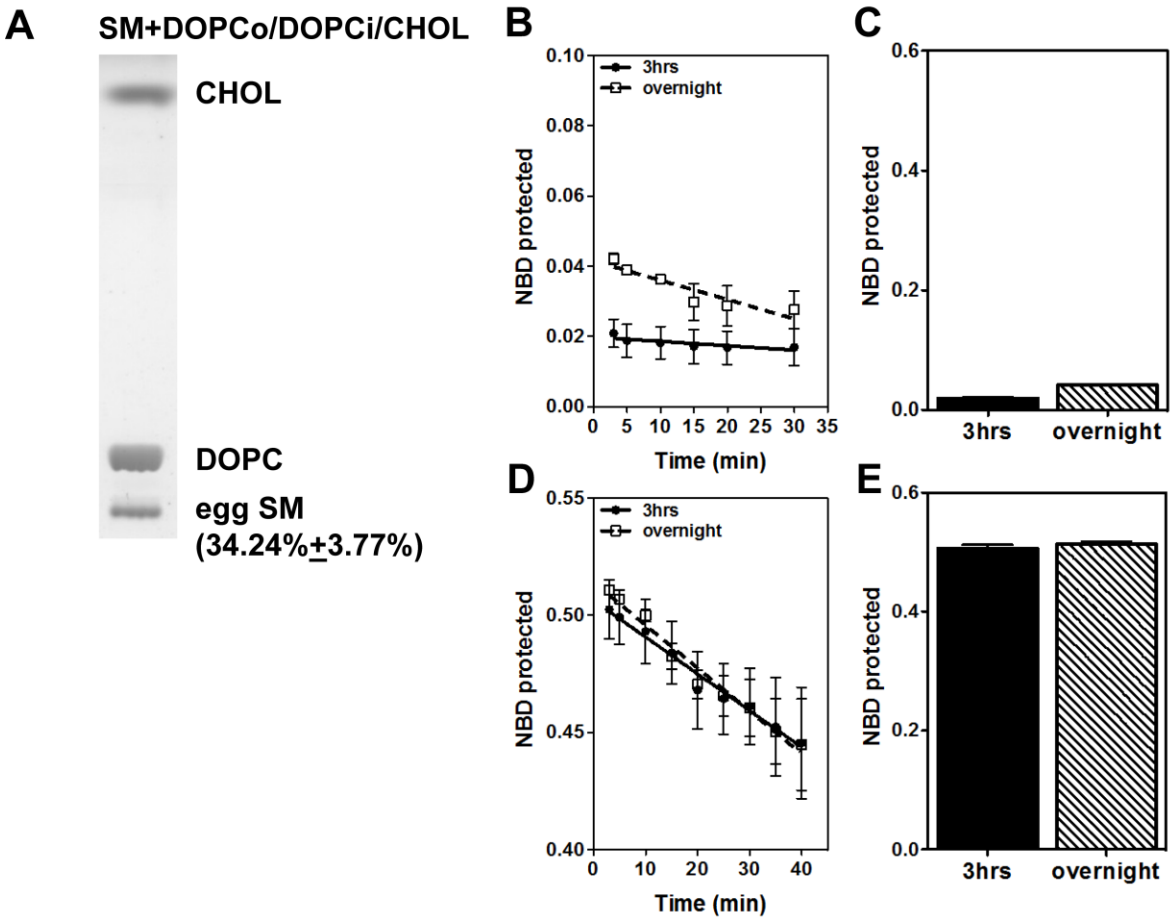

Supplementary Figure 2

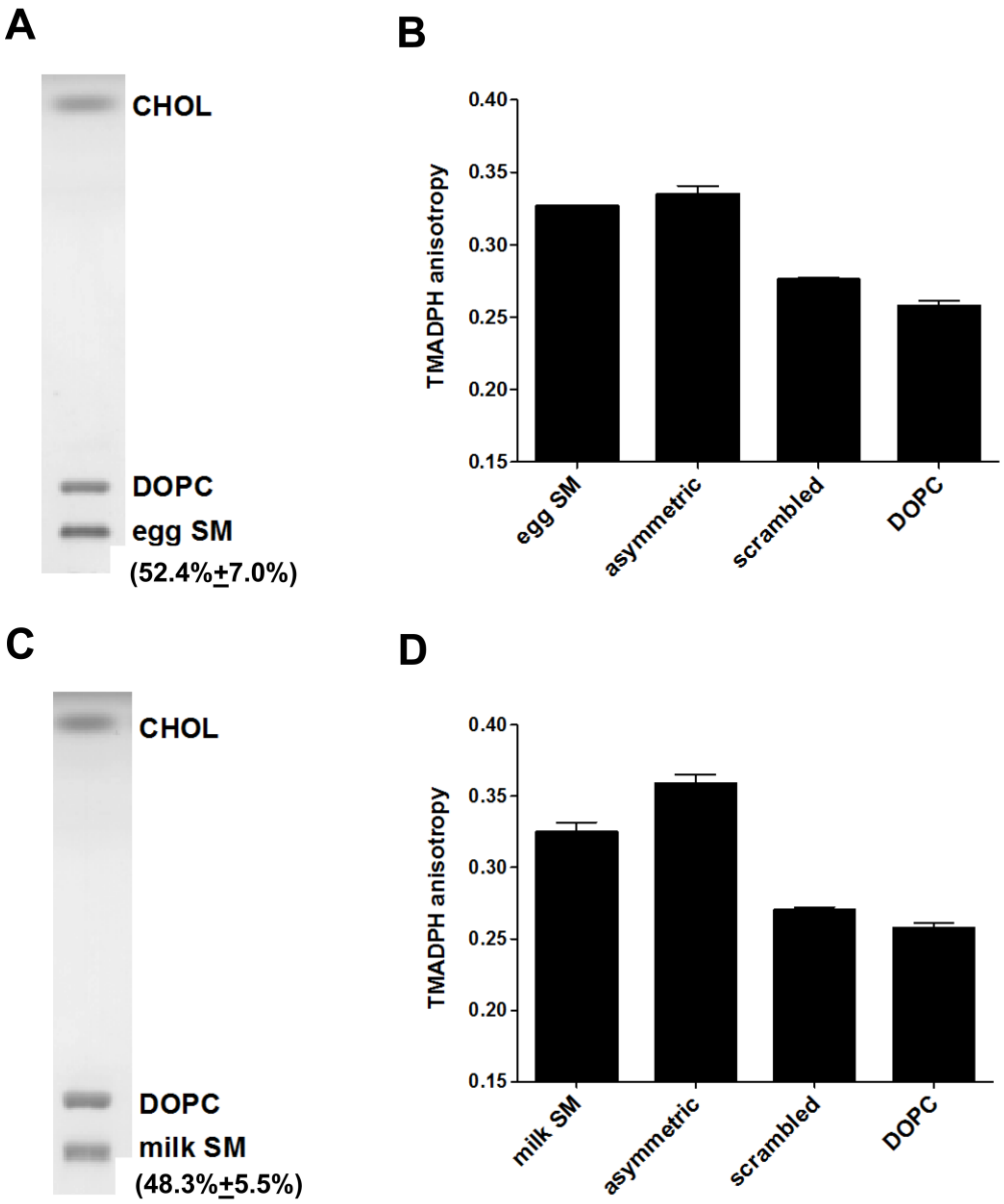

Supplementary Figure 3

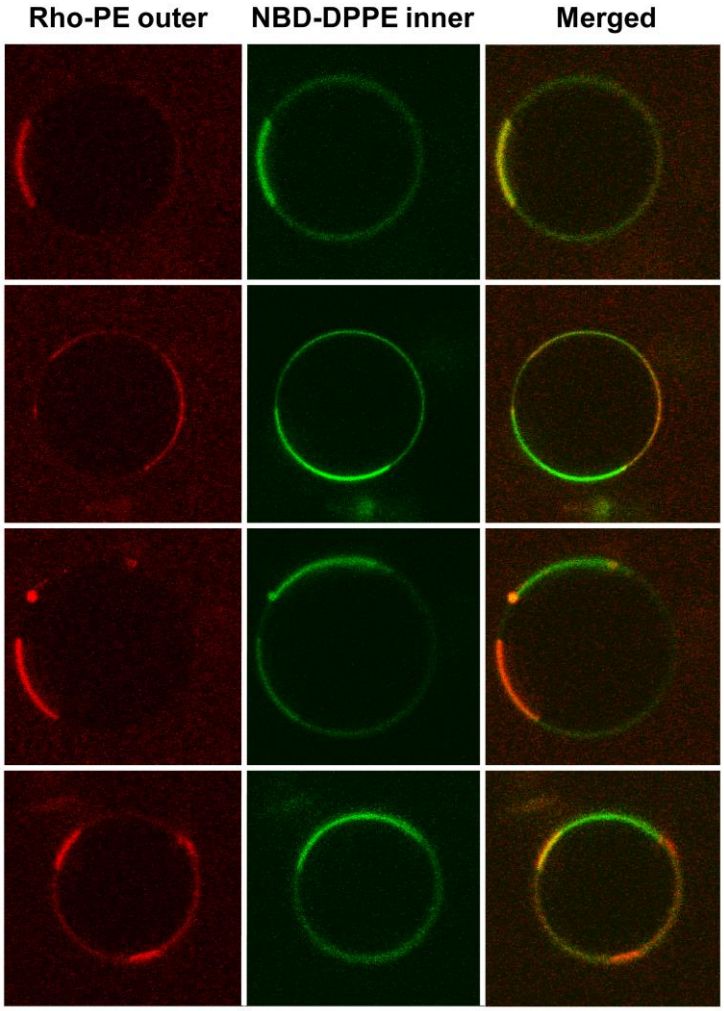

Supplementary Figure 4

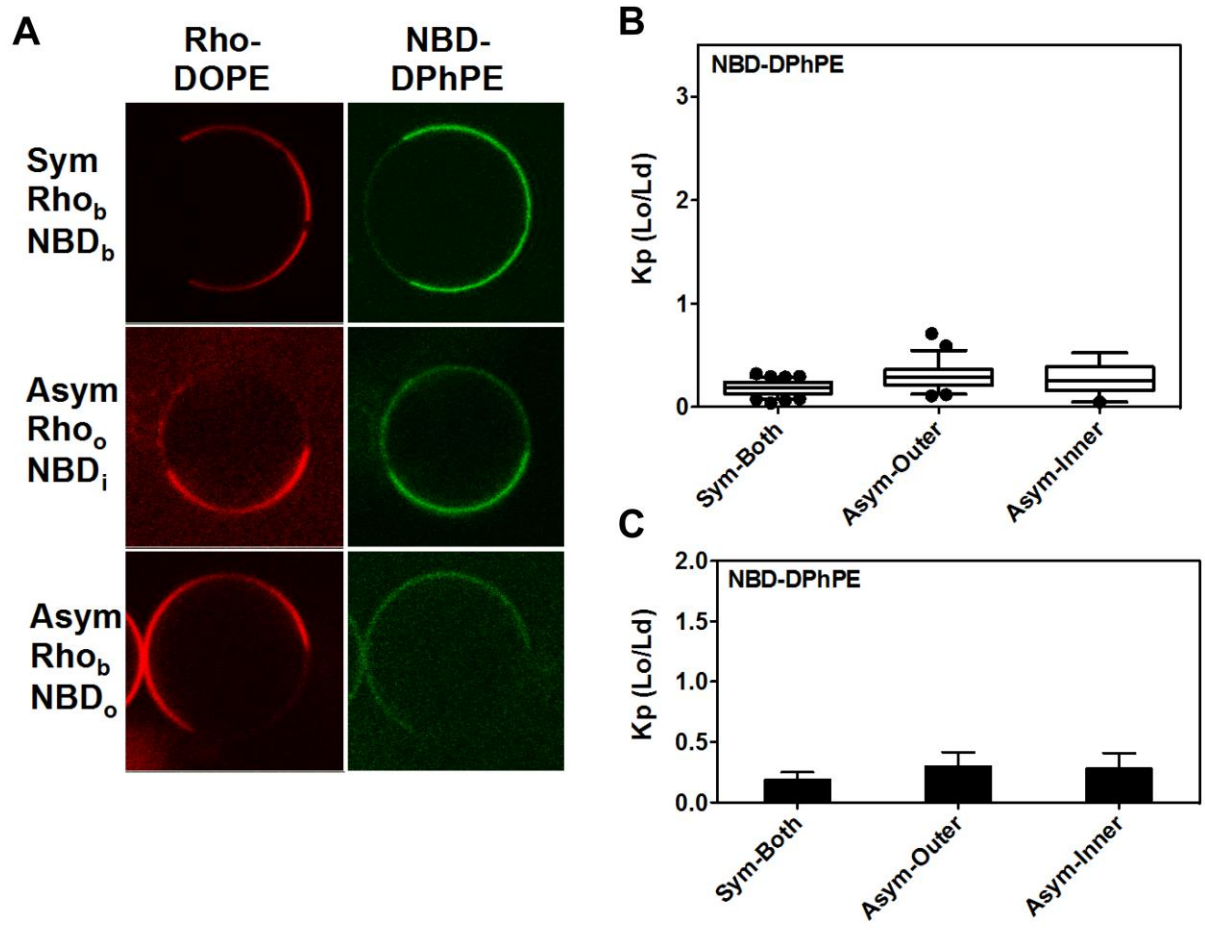

Supplementary Figure 5

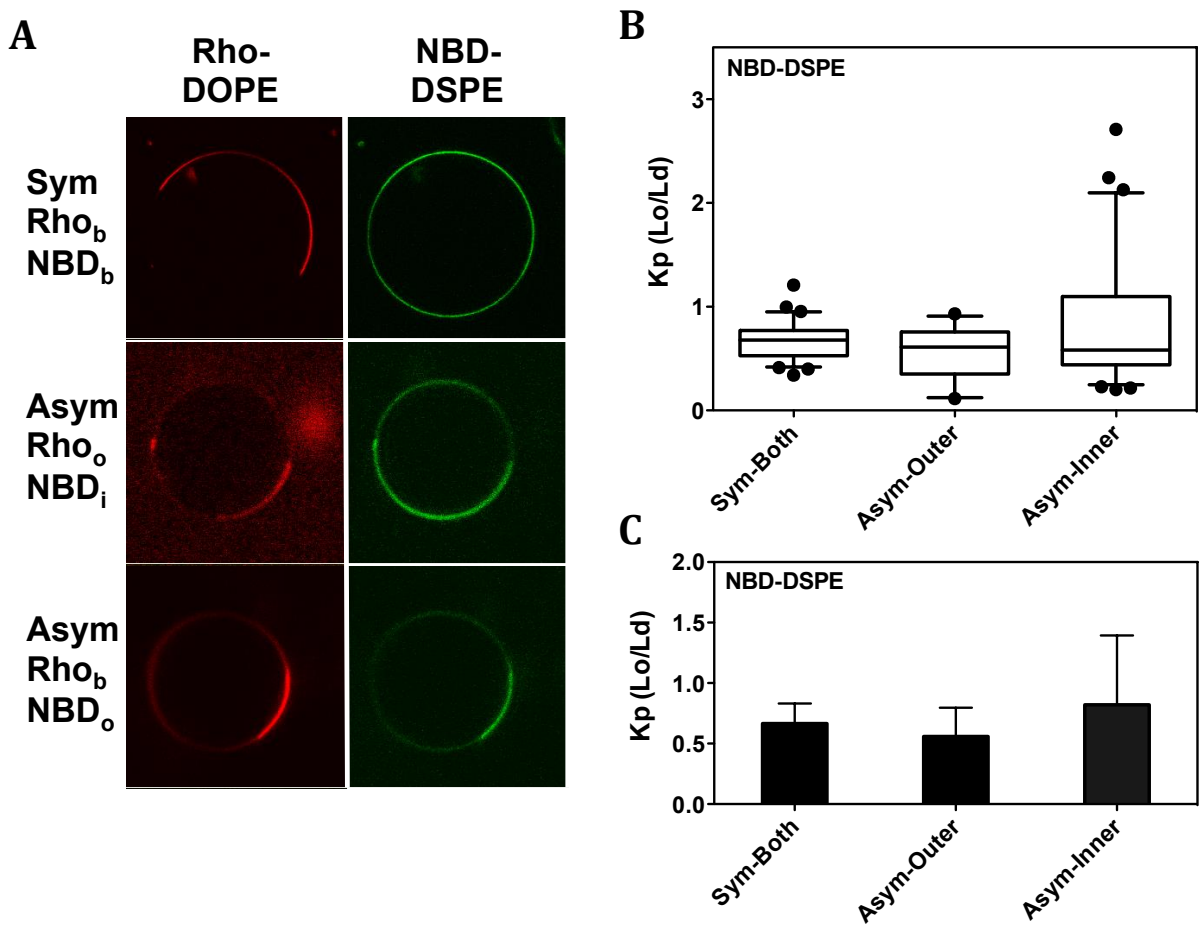

Supplementary Figure 6

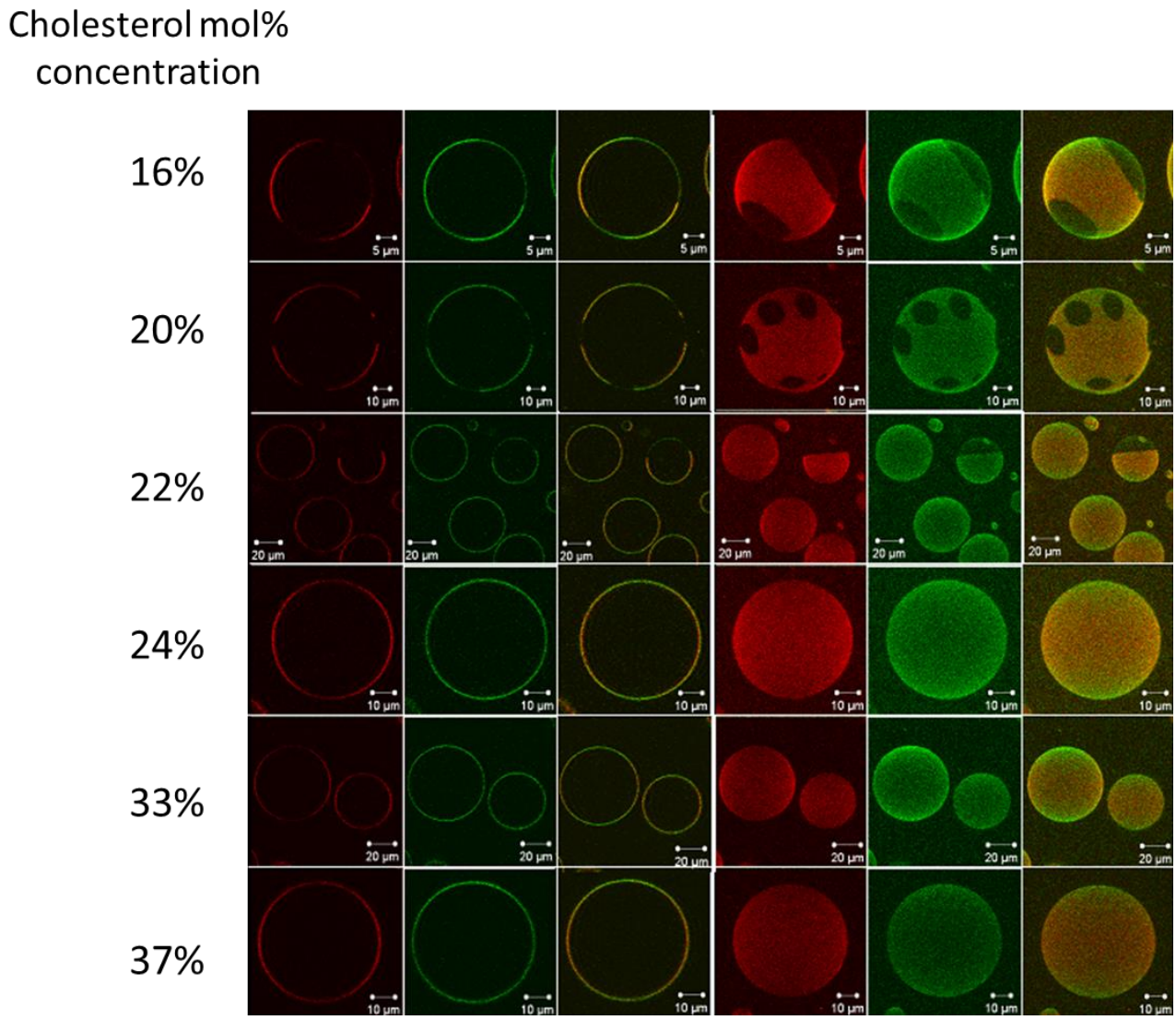

Supplementary Figure 7